Investigation of rare earth-doped BiAg high-temperature solders

**Yaowu Shi · Weiping Fang · Zhidong Xia ·
Yongping Lei · Fu Guo · Xiaoyan Li**

Abstract In the present work, the microstructure and properties of the rare earth Ce-doped BiAg solders with various Ag content are investigated. The results indicate that the maximum of the shear strength appears in the BiAg solder joints containing 5 and 7.5 wt.% Ag. At the same time, a similar trend appears in the hardness test of the BiAg bulk solders. Moreover, the results show that the microstructure and properties of the solders can be modified due to the unique properties of rare earth element. Small amounts of rare earth addition may enhance the wettability of SiAg solder on Cu substrate, and result in the increase of the shear strength of the solder joints. However, the rare earth addition may not give obvious influence on the melting temperature and the electrical conductivity. Thus, it is expected that the BiAg solder containing small amounts of rare earth element may possess a better potential as a replacement for high-Pb solders.

1 Introduction

High-temperature solders have been widely used to produce the reliable interconnections, in which the high-density packaging technology and high-service temperature are needed. The main applications include the air craft, space satellite, automotive, and oil/gas well exploration, etc. [1]. Nowadays, high-lead alloys are commonly used as high-temperature solders, because of their satisfactory properties, such as good wettability, high ductility, low shear modulus, etc. Moreover, high-lead solders generally provide much better resistance to thermo-mechanical fatigue.

Because of environmental reasons, the development of lead-free solders has become an important issue. Till now, however, only a few of candidates have been proposed for the lead-free high-temperature solders, such as AuSn, BiAg, and ZnAl-based alloys [2–6].

The Au20Sn eutectic alloy is considered as a potential lead-free high-temperature solder, because of its suitable melting temperature, good thermal and electrical conductivities, and good solderability [7]. Considering that the AuSn solder has brittle nature and high cost, the ZnAl based solder have recently been suggested as a potential candidate due to its low cost, small electrical resistivity, and good mechanical property [1]. However, the issues of wettability, brittleness, and corrosion still should be deeply studied for the ZnAl based alloys [8]. The BiAg system alloys exhibit an acceptable melting point, similar hardness to the Pb5Sn, and affordable cost. It has been developed as die attach solders for power devices and light-emitting diode. However, this solder alloy system is still under development, due to its inferior thermal and electrical conductivity and poorer workability. Recent investigation indicates that increasing the Ag content of the BiAg alloy to 11 wt.% promotes an increase in thermal conductivity and ductility [3, 4, 9]. Thus, a suitable Pb-free alternative has not yet been found up to now. Further development of high-temperature Pb-free solders is still needed.

It is well-known that the rare earth (RE) elements are surface-active elements, which play an important role in metallurgy of materials, such as refinement of microstructure, alloying and metamorphosis of inclusions. A

Y. Shi (✉) · W. Fang · Z. Xia · Y. Lei · F. Guo · X. Li
School of Materials Science and Engineering, Beijing University of Technology, 100 Ping Le Yuan, 100022 Chaoyang District, Beijing, China
e-mail: shiyw@bjut.edu.cn

minute amount of RE may greatly improve the properties of metals. Effect of RE addition on lead-free solder alloys has been widely studied by many researchers [10–12]. For a SnAgCu solder, minute amounts of rare earth can obviously improve the mechanical properties, extend the creep and creep-fatigue life of the solder joints [13, 14]. In addition the minute addition of RE can retard the degradation of joint strength under high temperature aging [15].

In the present work, the rare earth element-doped BiAg system alloys with various Ag contents are investigated with the aim of investigating the possibility for affecting the properties, which hinder the application of the BiAg solder as substitute for the lead-containing alloys.

2 Experimental procedures

The solder in this study was a BiAg system alloy with adding small amounts of rare earth. The adding amount of rare earth Ce was 0.1 wt.%. Moreover, for the sake of contrast, some RE-free BiAg solder alloys and Pb5Sn were prepared. The testing solder alloys are listed in Table 1.

Solder alloys were prepared by melting appropriate amounts of pure metals (>99.9% pure) in an Al_2O_3 ceramic crucible at about 550 °C for 30 min. With the help of a cast-iron bell with holes on the sidewall, the rare earth Ce was pushed down into the molten solder. After the rare earth Ce was melted, the molten alloy was held for 60 min and mechanically stirred every 20 min to promote homogeneity of the solder alloy. During the smelting, a eutectic salt KCl + LiCl with weight ratio of 1.3:1 was used over the surface of the liquid solder to protect the melt from oxidation. The molten solder was finally chill cast into a rod ingot (weight: 100 g, diameter: 10 mm) in a steel mold.

Melting temperature range of the solders was measured based on a Japanese Industrial Standard, JIS Z 3198-1: 2003 [16]. The starting temperature of melting was measured by the differential scanning calorimetry (DSC), and the starting temperature of solidification was measured by the cooling curve. The DSC samples that were 0.1 mm thick alloy pieces were cut from the alloy ingot. The heating rate was 2 °C/min with N_2 protection. The equipment for the DSC test is NETZSCH DSC 200 PC. The cooling curve was recorded with the help of a NiCr/NiSi thermocouple and ADAM-4018 measuring system software during solidification with slow cooling. Pure Pb (99.9 wt.%) was used for calibration.

For the spreading test, the substrate was Cu sheet with dimension of 40 mm × 40 mm × 0.3 mm. In the test a small solder ball (0.2 g weight) was used. After polishing, the substrate was degreased in a 50 % water solution of HCl, followed by cleaning in ethanol and drying in air. An activated flux was adopted, which consisted of $ZnCl_2$–NH_4Cl–H_2O. Reflow was conducted at 50 °C above liquidus for 15 s and cooled in air. After testing, the specimen was cleaned with acetone to remove the residue. The specimen was scanned into a computer along with a reference sample of known area. The spreading area of the solder was calculated through the function of "inquire" in AUTOCAD software. The wetting angles were measured from the centric cross-section of the spreading specimen under stereoscope. All the test results were an average of four specimens.

Shear strength of the solder joints was evaluated according to the Japanese Industrial Standard JIS Z 3198-5: 2003 [17]. Shear specimen is shown in Fig. 1. The solder joints were finished at 50 °C above liquidus of solder for 75 s in air with the aid of $ZnCl_2$–NH_4Cl flux. The shear test was conducted in a MTS810 electro-hydraulic servo tester at room temperature. The maximum loading capacity was 5 kN and loading speed was 0.05 mm/min. Microhardness measurement was taken under a 25 g load for 15 s using a HXD 1000 hardness tester. All the samples were with dimension of 18 mm × 3 mm × 3 mm, which were mechanically cut from the solder ingots. Surface of the samples was ground and polished.

Thermal and electrical conductivities are important properties for the high-temperature lead-free solder. Electrical
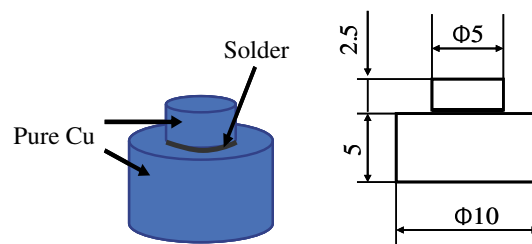
Fig. 1 Geometry of specimen (in mm)

Table 1 Compositions of the designated solder alloys (wt.%)

Series no.	1	2	3	4	5	6	7
Alloy	Bi2.5Ag	Bi2.5AgRE	Bi5AgRE	Bi7.5AgRE	Bi10Ag	Bi10AgRE	Pb5Sn

The percent of Bi and Ag was calculated after adding Ce

conductivity was measured on samples with dimension of 18 mm × 3 mm × 3 mm. The equipment used was a ZEM-2 type Seebeck and electrical conductivity instrument. The measurement was conducted at 70 °C with Ar gas protection.

For observation of microstructures, the samples were cut from the centric cross-section of the spreading specimen. The solder joint samples were etched slightly by using 4%HNO$_3$–96%C$_2$H$_5$OH solution for 3–5 s after grinding and polishing. Microstructure was observed under a scanning electron microscopy (SEM) equipped with an energy-dispersion X-ray spectrometer.

3 Results and discussion

3.1 Melting temperature

The test results are listed in Table 2. The results indicate that the liquidus temperature of the BiAg solders is increased with the increase of Ag content. The solidus of the BiAg solders remains almost stationary, and the value of the solidus is about 261 °C. That is, the melting temperature ranges become larger with the increase of Ag content. Moreover, the results indicate that with the addition of small amounts of rare earth Ce, the melting temperatures changed slightly. As indicated [3, 4], a Pb-free replacement for high Pb-solders must satisfy the solidus higher than 260 °C. Although the solidus of the BiAg

alloys is lower than that of Pb5Sn, the BiAg system alloys may fulfill this requirement.

3.2 Microstructure

Figure 2 shows the microstructure of Bi2.5Ag and Bi10Ag solder joints. The observation indicates that the Bi2.5Ag solder mainly consists of the fine BiAg eutectics. Primary Ag particles may be only found at several visual fields, and the particles are often located at the eutectic cell boundaries, because of the non-equilibrium solidification of soldering process. However, the Bi10Ag solder has a hypereutectic microstructure comprising dendritic primary Ag and BiAg eutectics. In addition, a Cu-rich phase with an acicular morphology can be observed. Based on a EDX analysis, the Cu-rich phase has a composition of Cu-40at.%Bi-4at.%Ag. Formation of the Cu-rich phase is because of the diffusion of Cu into the solder. From the observation at interfaces between the BiAg solder and substrate, it is indicated that there is no interfacial reaction product. It is felt that there is no metallurgical reaction at the interface between the solder and substrate. There only exists mechanical joining at the interface. In addition, it is clear that many Ag-rich phases can be found in solder side at the interface, as shown in Fig. 2b and c.

Figure 3 shows the effect of different Ag contents and rare earth element addition on microstructure of BiAg solder joints. It is indicated that the dendritic primary Ag and acicular Cu-rich phase in the solder is gradually increased with the increase of Ag content. Moreover, it is found that the constituents of the microstructure of the BiAg solders have no obvious change, when small amounts of rare earth are added in the solder. However, the RE addition can somewhat refine the microstructure of solders. Especially, the acicular Cu-rich phase and the coarse Ag-rich phase are obviously refined. Needle- or slice-like structure is shortened. Thus, with the addition of small amounts of RE elements, the more uniform microstructure is generated for the BiAg solders. Similar phenomenon

Table 2 Melting temperature of Bi-Ag and Pb5Sn solders

| Solder	Liquidus (°C)	Solidus (°C)
Bi2.5Ag	262.6	260.9
Bi2.5AgRE	262.3	260.9
Bi5AgRE	301.5	260.9
Bi7.5AgRE	334.5	260.7
Bi10Ag	380.6	261.4
Bi10AgRE	378.2	260.8
Pb5Sn	311.6	310.6
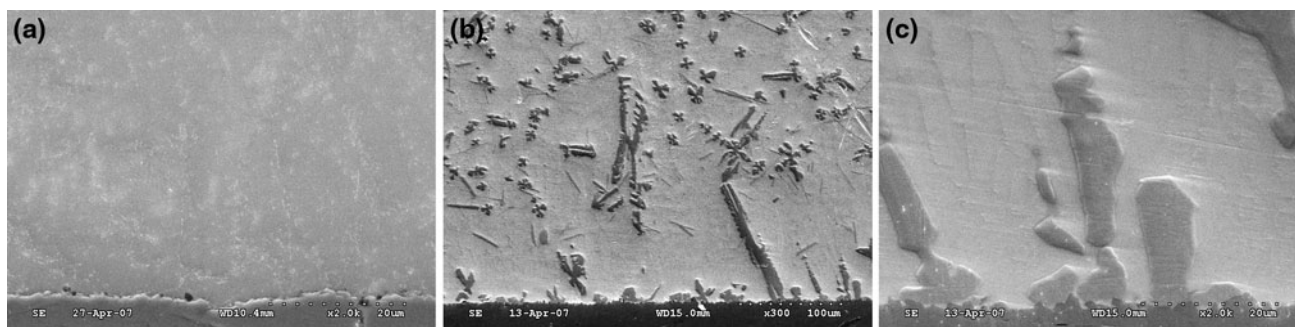
Fig. 2 Microstructure of BiAg solder joints. **a** Bi2.5Ag, **b** Bi10Ag, **c** Bi10Ag with high magnification

Fig. 3 Effect of rare earth
addition on microstructure of
BiAg solder joints.
a Bi2.5AgRE, **b** Bi5AgRE,
c Bi7.5AgRE, **d** Bi10AgRE
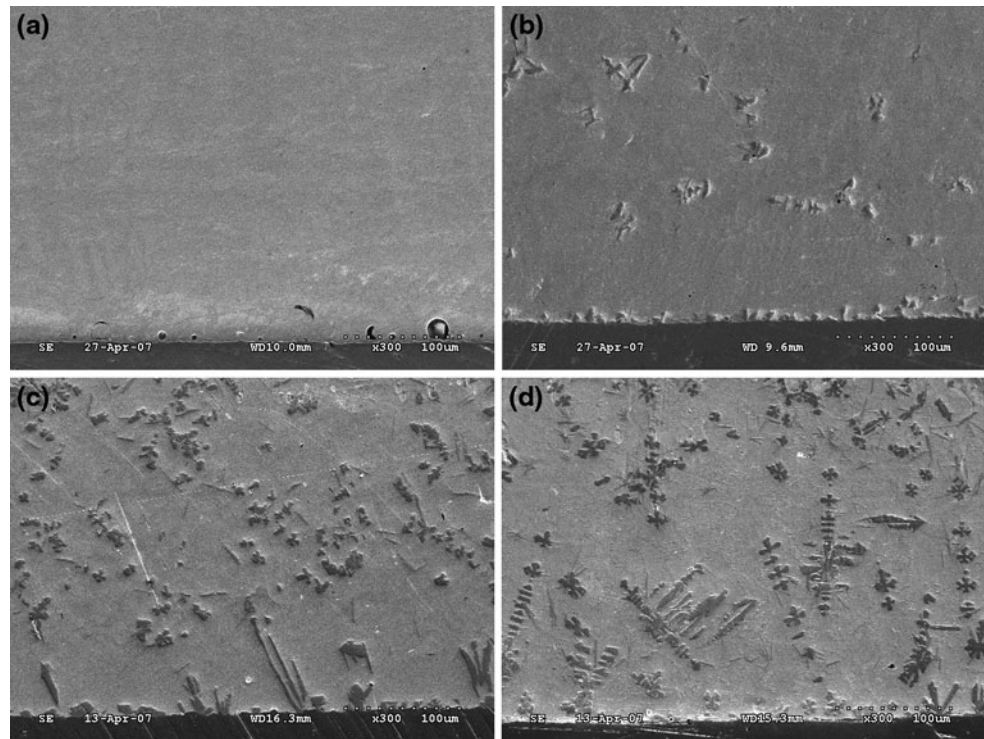
appears in Sn-based solders, such as SnAgCu [11], SnAgBi
[18], and SnBi [19]. The reason is due to the unique
properties of RE elements. As surface-active elements, the
adsorption phenomenon plays an important role during
solidification of alloys and may greatly affect their
microstructure [12, 20]. During solidification, RE may
agglomerate at the interfaces of the primary phases and at
the grain boundaries. The decrease of the interface energy
would refine the size of grains.
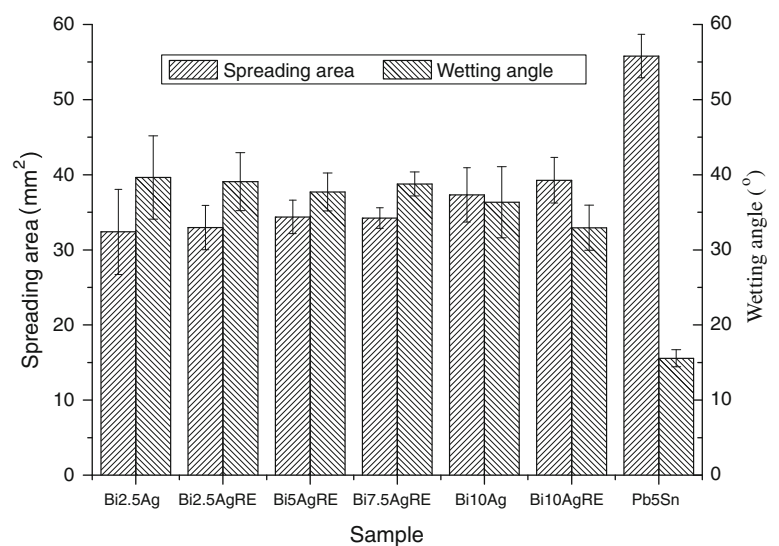
3.3 Wettability

Results of spreading test reflect the wettability of solder on
a substrate under a certain environment. The wettability is
an important property related to the soldering technology.
Figure 4 shows the spreading area and wetting angle of the
BiAg alloy solders in the test. The results are an average of
four tests for each solder. It is indicated that the wettability
of SiAg solder on Cu substrate is fair, but it is still inferior

Fig. 4 Spreading area and
wetting angle of the BiAg alloy
solders

to the Pb5Sn solder. An increase in the Ag content of solder has a positive effect on the wettability to Cu substrate. That is, with the increase of Ag content, the spreading area increases and the wetting angle decreases. Moreover, it is clear that the RE addition may promote the wetting property. The reason is related with the surface-active action of rare earth elements. The rare earth elements make interfacial surface energy decreased. The decrease of the interfacial tension then makes the wetting angle between the solder and substrate lowered, and the spreading of the solder increased. In addition, spreading of solder may be enhanced, if the solder possesses a highly refined grain size [21, 22]. The fine grain structure helps promote uniform and rapid melting as the temperature of the solder is raised because the discrete phases are finely divided and the alloy tends toward homogeneity.

3.4 Mechanical properties

Figure 5 shows the microhardness of the bulk solder. It is indicated that the hardness of BiAg solders is obviously higher than that of the Pb5Sn solder. In addition, it is felt that the maximum of the hardness appears in the solders containing 5 and 7.5 wt.% Ag. The test indicates that the trace RE addition results in the increase of the hardness.

The shear strength of solder joints shows a trend of initial rise up to 7.5 wt.%Ag, then drop for 10 wt.% Ag, as shown in Fig. 6. It is expected that the maximum of the shear strength appears in the solders containing 5–7.5 wt.% Ag. The maximum value of the shear strength may be related to a suitable fraction of the primary Ag phases existed in the solder alloys. It is known that the shear modulus, G, of pure metal, Ag, Bi, and solder Bi11Ag is 30.3GPa, 12GPa, and 13.28GPa, respectively [3, 23]. The elastic constants of solder alloys containing 2.5–7 wt.%Ag
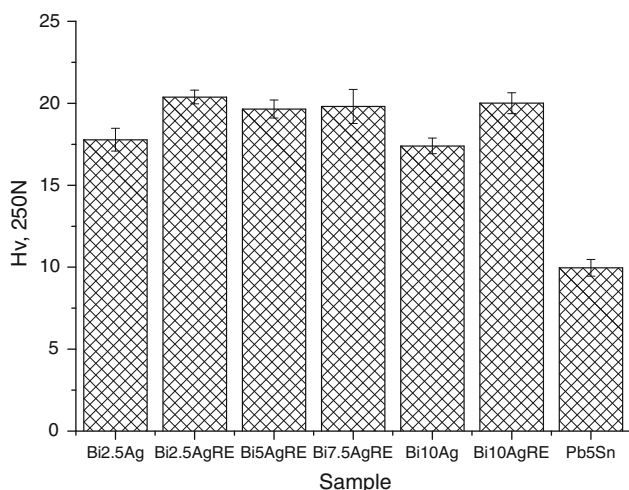
Fig. 5 Microhardness of bulk solders
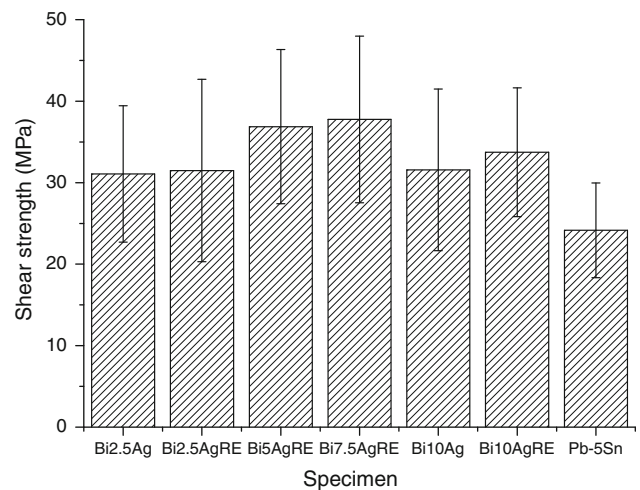
Fig. 6 Shear strength of solder joints

can be reasonably estimated from atomic properties of the constituent elements. Obviously, the Ag phase may be considered as a strengthening phase. It is expected that the strengthening effect of Ag phase would increase with the increase of Ag content. However, the maximum strengthening effect appears in solders containing 5–7.5 wt.% Ag. It expected that superfluous Ag would lead to deteriorate the properties of solder.

Similar results are found in the composite solders reinforced by nano- and micro-sized particles. For example, the influence of single-wall carbon nanotube (SWCNT) addition on the microstructural and tensile properties of SnPb solder alloy is investigated, in which the single-wall carbon nanotube is considered as a strengthening phase [24]. It is found that the maximum strength attained at 0.3 wt.% of the SWCNT reinforcement, nearly 18% higher than that of SnPb eutectic solder matrix. That is, the values of the ultimate tensile strength (UTS) increase from 52.5 MPa of un-reinforced solder to 66.1 MPa for the composite solder with the addition of 0.3 wt.% SWCNT. Also, it is found that an addition of 0.5 wt.% SWCNT results in a remarkable decrease in UTS. The enhancement of the strength of composite solders is ascribed to the presence and distribution of fine strengthening particles within the matrices and at the grain boundaries of solder, which tend to alter the deformation characteristics of solder alloys by impeding grain-boundary sliding while concurrently retarding dislocation movement in solder matrices. Higher content of the SWCNT results in the bad dispersion and aggregation, which may explain the decline of the strength of the composites beyond 0.3 wt.%.

It is found from the shear test that the fracture of all the BiAg solder joints occurs at the interface of joints, as there is no interfacial intermetallics which could enhance interfacial bonding. Thus, the BiAg solder may result in weaker

bounding of the joints. Moreover, it is not found that the liquid BiAg solder grooves and even penetrates the grain boundaries of Cu substrate, because the soldering time is rather short for the preparation of the solder joint coupon in this investigation. In addition, the tests indicate that adding small amounts of rare earth elements may increase the shear strength of the BiAg solder joints. The reason may be related to the refinement of microstructure due to the RE addition. The uniform microstructure is then able to promote the hardness and shear strength.

3.5 Electrical conductivity

It is well-known that solder alloys are used as the interconnecting materials in electronic packaging. Solder joints provide both the electrical and mechanical connections in electronic packaging modules. Thus, the electrical conductivity of BiAg solders is measured. The value of the electrical conductivity for each solder is an average of 16 measurements. The results are shown in Fig. 7. It is indicated that the conductivity of the solder is slightly increased with the increase of Ag content because of the good electrical conductivity of Ag. However, the electrical conductivity of BiAg solders is still inferior to that of the high-lead solder. The conductivity of BiAg solders is about one third of the Pb5Sn high-lead solder. In addition, it is found that the trace RE additions do not give obvious influence on the electrical conductivity of the BiAg solders.

4 Conclusions

The rare earth element-doped BiAg solders with various Ag content are investigated, and the results shows the microstructure and properties can be modified due to the
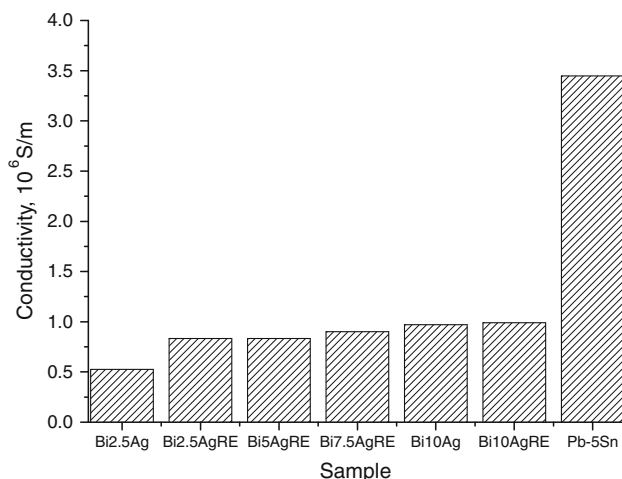
Fig. 7 Electrical conductivity of solders

unique properties of rare earth element. The BiAg solder containing small amounts of rare earth element may possess a better potential as a replacement for high-Pb solders. The main results are summarized as follows:

1. The maximum of the shear strength appears in the solder joints containing 5 and 7.5 wt.% Ag. A similar trend appears in the hardness test results of the BiAg bulk solders.
2. Small amounts of rare earth addition may enhance the wettability of BiAg solders on Cu substrate. At the same time, the rare earth addition results in the increase of the shear strength.
3. Small amounts of rare earth addition may not give obvious influence on the melting temperature and the electrical conductivity.

References

1. N. Kang, H.S. Na, S.J. Kim, C.Y. Kang, J. Alloys Compd. **467**, 246–250 (2009)
2. M. Rettenmayr, P. Lambracht, B. Kempt, C. Tschudin, J. Electron. Mater. **31**, 278–285 (2002)
3. J.N. Lalena, N.F. Dean, M.W. Weiser, J. Electron. Mater. **31**, 1244–1249 (2002)
4. J.M. Song, H.Y. Chuang, Z.M. Wu, J. Electron. Mater. **35**, 1041–1049 (2006)
5. Y. Takaku, L. Felicia, I. Ohnuma, R. Kainuma, K. Ishida, J. Electron. Mater. **37**, 314–323 (2008)
6. W. Fang, Y. Shi, Z. Xia, Y. Lei, F. Guo, Electron. Compon. Mater. **28**, 71–73 (2009)
7. G. Matijasevic, C. Wang, C. Lee, IEEE Trans. Comp. Hybrids Manuf. Technol. **13**, 1128–1134 (1990)
8. T. Shimizu, H. Ishikawa, I. Ohnuma, K. Ishida, J. Electron. Mater. **28**, 1172–1175 (1999)
9. W. Fang, Y. Shi, Z. Xia, F. Guo, Y. Lei, Electron. Compon. Mater. **27**, 15–18 (2008)
10. Z. Xia, Z. Chen, Y. Shi, N. Mu, N. Sun, J. Electron. Mater. **31**, 564–567 (2002)
11. Z.G. Chen, Y.W. Shi, Z.D. Xia, Y.F. Yan, J. Electron. Mater. **31**, 1122–1128 (2002)
12. C.M.L. Wu, Y.W. Wong, J. Mater. Sci. Mater. Electron. **18**, 77–91 (2007)
13. Z.G. Chen, Y.W. Shi, Z.D. Xia, Y.F. Yan, J. Electron. Mater. **32**, 235–243 (2003)
14. W. Xiao, Y. Shi, G. Xu, R. Ren, F. Guo, Z. Xia, Y. Lei, J. Alloys Compd. **472**, 198–202 (2009)
15. G. Li, Y. Shi, H. Hao, Z. Xia, Y. Lei, F. Guo, X. Li, J. Mater. Sci. Mater. Electron. **20**, 186–192 (2009)
16. JIS Z 3198-1, Test methods for lead-free solders, Part 1: methods for measuring of melting temperature ranges, Japanese Industrial Standards Committee, 2003
17. JIS Z 3198-5, Test methods for lead-free solders, Part 5: methods for tensile tests and shear tests on solder joints, Japanese Industrial Standards Committee, 2003

18. Z. Xia, Z. Chen, Y. Shi, N. Mu, N. Sun, J. Electron. Mater. **31**, 564–567 (2002)
19. W. Dong, Y. Shi, Z. Xia, Y. Lei, F. Guo, J. Electron. Mater. **37**, 982–991 (2008)
20. Z. Zhang, Physicochemistry of materials (Chemical Industry Press, 2006), p. 163
21. D.M. Jacobson, G. Humpston, S.P.S. Sangha, Weld. J. **75**, 243s–250s (1996)
22. Y. Shi, Y. Yu, Y. Li, Z. Xia, Y. Lei, X. Li, F. Guo, J. Mater. Eng. Perform. **18**, 278–281 (2009)
23. R.W. Hertzburg, *Deformation and fracture mechanics of engineering materials*, 4th edn. (J. Wiley & Sons, New York, 1996)
24. K.M. Kumar, V. Kripesh, A.A.O. Tay, J. Alloys Compd. **455**, 148–158 (2008)